International Journal of Smart Grid (IJSmartGrid)
https://www.ijsmartgrid.org/ Online ISSN: 2602-439X
K. Natarajan et al., Vol. 10, No. 2, June, 2026 Research Article

Enhanced Power Quality in Solar PV-Based Unified Active Power Filters using a High-Gain Boost-Luo Converter with Intelligent Control

K. Natarajan*‡, Mohammadha Hussaini M**, Siddheswar Kar***, Krishna Prakash Arunachalam****, Pranita Chavan*****, S. Baskaran******

*Professor, Department of Electrical and Electronics Eng., Trinity College of Engineering and Technology, Peddapalli, India.

**Assoc. Professor, Department of Electrical and Electronics Eng., Government College of Eng., Erode, Tamilnadu, India.

***Assistant Professor, Department of Electrical Engineering, Medicaps University, Indore, India.

****Departamento de Ciencias de la Construcción, Facultad de Ciencias de la Construcción Ordenamiento Territorial, Universidad Tecnológica Metropolitana, Santiago, Chile, 8330383.

*****Assistant Professor, Pillai HOC College of Eng. and Technology, Rasayani, University of Mumbai, 410207, India.

******Associate Professor, Department of Electrical and Electronics Engineering, Saveetha School of Engineering, Saveetha Institute of Medical and Technical Sciences, SIMATS, Saveetha University, Chennai, Tamilnadu, India.

(drknatarajan17@gmail.com, hussaini1008@gmail.com, siddheshwar.kar@medicaps.ac.in, k.prakash@utem.cl, pranitapramod44@gmail.com, baskaran1985@gmail.com)

‡Corresponding Author; K. Natarajan, drknatarajan17@gmail.com

Received: 14.07.2025 Accepted: 13.03.2026

Abstract- Maintaining high power quality is essential in modern electrical systems, as even minor distortions significantly impact equipment performance, operational efficiency and system reliability. Power Quality (PQ) issues such as harmonic distortion, voltage instability and frequency deviations pose major challenges to smooth operation of electrical networks. The integration of Renewable Energy Sources (RESs), particularly Photovoltaic (PV) systems, further complicates PQ management due to their intermittent nature. To address these challenges, this research proposes a Unified Active Power Filter (UAPF) that combines both series and shunt compensation techniques for comprehensive PQ enhancement. A PV based High-Gain Integrated Boost-Luo Converter is incorporated to power the DC link while an Improved Artificial Rabbit Optimized Proportional-Integral (IARO-PI) controller ensures precise voltage regulation and stable DC-link voltage. Additionally, a Cascaded Fuzzy Controller governs UAPF operation, enabling adaptive responses under nonlinear and dynamic system conditions. The proposed PV-UAPF system is validated through MATLAB simulations, achieving a substantial reduction in Total Harmonic Distortion (THD) to 0.98% and maintaining near-unity power factor. These results confirm that the integration of renewable energy with intelligent PQ management provides a robust solution for delivering stable, efficient and sustainable power distribution.

Keywords - Power quality, renewable energy sources, unified active power filter, high gain integrated Boost-Luo converter, IARO-PI controller, cascaded fuzzy controller.

Cite this article as: K. Natarajan, M. Hussaini M, S. Kar, K.P. Arunachalam, P. Chavan, and S. Baskaran, "Enhanced Power Quality in Solar PV-Based Unified Active Power Filters using a High-Gain Boost-Luo Converter with Intelligent Control" *International Journal of Smart Grid (ijSmartGrid)*, Vol. 10, No. 2, pp. 73-84, June, 2026.

1. Introduction

PQ issues are increasingly prevalent in modern electrical systems owing to the extensive usage of linear and non-linear loads [1].These issues, as displayed in Figure 1 manifest as disturbances such as voltage sags, harmonics, flicker and unbalanced current, which significantly affect the performance and reliability of sensitive equipment. In order to conquer these challenges, the researchers have developed a number of ways to enhance PQ by utilizing Power Factor Correction (PFC) devices [2-3]. PFC techniques are pivotal in enhancing the efficiency and reliability of electrical systems by addressing inefficiencies associated with low power factors [4]. The large scale projects and installations typically utilize specialized equipment, such as Dynamic Voltage Resistor (DVR), Unified Power Quality Conditioners (UPQC) and distribution Static Synchronous Compensators (D-STATCOM) [5-6]. These devices are also known as Unified Active Power Filter, which is a sophisticated device employed in this developed work to significantly improve PQ by actively compensating for a range of disturbances and harmonics [7]. Conventional filters lacks the ability to adapt to dynamic changes in load characteristics and network conditions, which leads to inadequate power compensation for varying PQ disturbances [8]. These drawbacks are overcome by the UPAF system, which integrates both series and shunt active filter. The UAPF integrates both series and shunt active filters: the series filter regulates voltage by compensating sags and swells, while the shunt filter mitigates harmonic currents in real time. Together, they enhance PQ and improve system reliability. By combining these functionalities, UAPF provides an effective solution to enhance PQ, reduce energy losses and extend the lifespan of load.

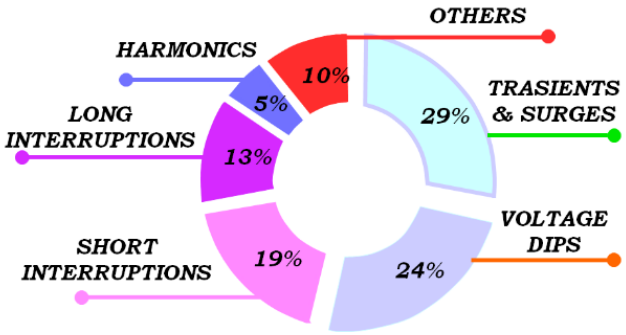


Fig. 1. Major PQ issues studied in Ref [9].

Furthermore, the control technique is essential for UAPF to enhance the reliability, efficiency and adaptability of the electrical network, this is also crucial in modern power system where the demand for stable and high quality electrical supply is paramount [10]. The conventional control technique is widely used in UAPF system due to their ability to provide desired performance metrics such as harmonic mitigation and PFC and it is robust in handling linear system dynamics. However, it is limited in handling non-linearity's and sudden changes in system dynamics without additional enhancements [11]. Therefore, the intelligent control technique of fuzzy controller [12] is employed to control the UAPF system efficiently. This control technique adapt their control actions based on real time inputs, mimicking human decision-making processes. Nevertheless, this method has computational demands, which impact real-time control performance and system responsiveness [13-14]. Henceforth, the proposed work introduced a cascaded Fuzzy controller, which ensuring the UAPF effectively filters out harmonics and regulated PF with high accuracy.

The UAPF interconnected with the DC-link, to power this RES based PV system is utilized for reducing the greenhouse emission, which generate low output voltage owing to its sporadic nature [15]. Therefore, the DC-DC converter is required for maximizing the power of PV system, thus conventional boost, Cuk, SEPIC and Luo converter is developed for enhancing the output voltage of PV with refaces the challenges like switching stress, high complexity, and low efficiency with ripple current [16-17]. Henceforth, the proposed study introduces a novel interleaved Boost-Luo converter for providing high voltage gain with reduced switching stress. This converter enhance the voltage, but it not generate stabilized voltage, thus the control technique needs to be implement [18]. The PI controller generally used to control the voltage and to tune the parameters of this controller, Improved Artificial Rabbit Optimization approach is developed in this study for providing better performance with quick settling time and convergence speed.

Literature Survey:

Surya Prakash *et al* (2025) [19] have presented an Adaptive Proportional Integral Controller (API) for PV based Shunt Active Power Filters (SAPF). The API controller adaptively modify its parameters based on the dc-link error voltage and therefore support low bandwidth disturbance rejection for high speed dynamic response with reduced settling time, while suppressing high-order harmonic currents from the utility grid. However, the performance of the API controller is contingent on its ability to accurately estimate the reference currents.

Sergio Coelho *et al* (2022) [20] have introduced a Unified Power Converter (UPC) for solar PV in microgrid systems. The UPC function in four operating modes and each of these operating modes utilizes Dual Phase-Shifting (DPS) Modulation implemented through a Dual Active Bridge (DAB), which provides galvanic isolation and bidirectional power flow. Nonetheless, the use of high switching frequencies (100kHz), increase the difficulty of accurately calculating components.

Rajendran Boopathi *et al* (2025) [21] have implemented Predictive Direct Power Control (PDPC) approach for PV interfaced shunt active power filter. PDPC method generates reference input signals for three-level NPC inverters, providing effective harmonic reduction, reactive power compensation and active power production from the PV arrays which results in enhanced overall quality of the grid supplied power. Complex algorithm implementation creates increased computational weight that impede real time adaptation of the controller under a highly dynamic non-linear load.

V. Sheeja *et al* (2023) [22] have developed a non-isolated High Gain Boost Converter (HGBC) for compensating reactive harmonics in the grid. The HGBC which employs a sliding mode power flow controller and frequency-adaptive (SOGI) control for effective reactive power compensation and harmonic current compensation. Yet, the HGBC has designed for operation at very low voltages to minimize switch stress.

K. Hemasri *et al* (2024) [23] have designed a fuzzy controller for reducing harmonics in SAPF. The fuzzy logic controller is effective for mitigating harmonics and creates reactive power compensation for unbalanced loads while keeping the THD of the source current within the IEEE-519 limit of 4.74%. However, it relies heavily on the well-designed rule base and finely tuned parameters.

Problem Definition:

In modern electrical systems PQ issues are serious issues such as harmonics, voltage sags and unbalanced currents especially due to the widespread use of nonlinear loads. Typical controllers and filters does not adapt to the dynamic variations of the load, which results in poor compensation and a drop in efficiency. Besides this, PV-based systems are characterized by low and fluctuating voltage outputs, while the use of traditional converters causes switching stress and ripple. Hence, an advanced technique is necessary to accomplish efficient harmonic elimination, stable voltage regulation, and improved grid reliability.

The implemented work foremost contributions are illustrated as below,

- The UAPF plays a vital role in this work for enhancing PQ by addressing harmonic distortions, improving PF and balancing loads.
- Implementing Cascaded Fuzzy controller to effectively manage the operation of UAPF.
- A novel PV based Interleaved Boost-Cuk converter is introduced to ensures the voltage from the PV array matches the requirements of the DC-link.
- Employing Improved ARO optimized PI controller to enhance the voltage control, achieve fast response time with minimized MSE.

Organization:

Section 2 details proposed UAPF system description. Section 3 provides a comprehensive methodology, including all modeling of the UAPF System, fuzzy controller in cascade, PV system, boost-luo converter and improved rabbit optimization technique. Section 3 outline simulation results and performance analysis. Finally, Section 4 provide concluding remarks, including major findings and other contributions.

2. Proposed System Description

In modern power system, the PQ issues are progressively prominent due to the widespread usage of linear and non-linear loads. Challenges such as voltage fluctuations, harmonics, voltage swell and sag. To address these challenges, the UAPF is developed in this work, which combines the capabilities of both series and shunt active power filter that efficiently mitigate the harmonic distortions and enhance the overall PQ in the linear and non-linear load. Moreover, to power DC-link of UAPF the proposed work introduced PV fed Interleaved Boost-Luo converter with Improved ARO optimized PI controller. The block diagram of the developed work is illustrated in Figure 2 as follows.

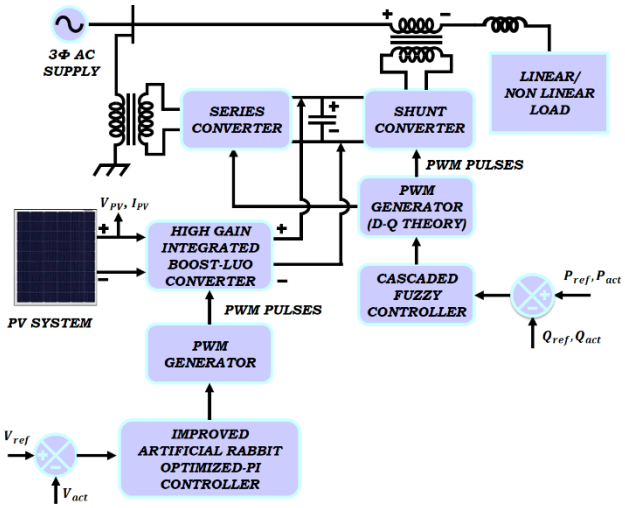


Fig. 2. Block diagram of the proposed work.

The three phase AC supply is linked with the linear and linear load, the UAPF, which is the combination of series and shunt active filters are connected in series and parallel across the PCC to control the voltage and current compensation. The UAPF consist of DC-link capacitor in between the series and shunt converter. To power the DC-link of UAPF, the RES based PV system is employed. The PV system convert the sunlight into electricity, due to the ecological changes it provide low output voltage, to boost low output in to require level it is given to the Interleaved Boost-Luo converter. This converter efficiently enhances PV voltage with high voltage gain and reduced switching stresses. Subsequently, the obtained actual voltage is compared with the reference voltage, which generate an error signal it is fed to the PI controller for error compensation thereby the stabilized voltage is attained. Moreover, to provide the stable output with less settling time, the PI controller's parameters are tuned with the aid of Improved ARO algorithm. The PWM generator is employed to provide the essential pulses for better switching operation of the converter, which is delivered to the DC-link of the UAPF. Subsequently, the UAPF is controlled by the Cascaded Fuzzy controller and to generate the appropriate pulses for the UAPF, the PWM generator (DQ theory) is utilized. Thereby, the reduced THD and stabilized power is delivered to the linear/non-linear load through the UAPF.

3. Proposed System Methodology

3.1. Modelling of UAPF System

In this work, to efficiently mitigate the PQ issues in linear and non-linear load, the UAPF is employed and the Figure 3 illustrates the diagram of UAPF system. The system consists of several key components that work together to improve the

Q delivered to industrial loads. The transmission system generates and supplies electrical power to the utility where the power enters the distribution network of the point of common coupling (PCC) the UPAF system is integrated. This point is crucial as it represents the junction where the utility's power meets the power systems of the industrial loads. The UF system includes two main active filters, the series active filter and the shunt active filter, both of which are interconnected through a DC-link. The series active filter is responsible for mitigating voltage based distortions and compensating for any voltage sags, swells or harmonics that affects the PQ. It ensures that the voltage supplied to the industrial loads is stable and within acceptable quality standards.

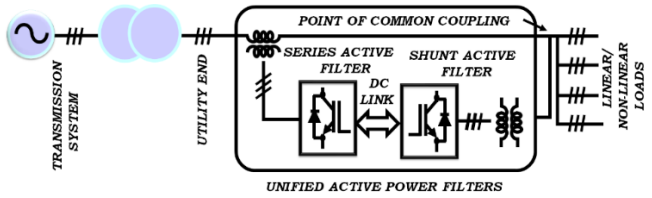


Fig. 3. Structure of UAPF.

Moreover, the shunt active filter is designed to address current based issues, such as harmonics current produced by non-linear loads and reactive power compensation. It aids to maintain a balanced and pure current flow from power compensation.it helps to maintain a balanced and pure current flow from the PCC to the industrial loads. By dynamically adjusting to the load conditions the shunt active filter maximized current distortion and enhance the overall power factor. Together, these filters ensure that the power supplied to the industrial loads is of high quality, free from significant distortions and inefficiencies. The DC-link between the two filters facilitates the exchange of energy, enabling coordinated operation for optimal PQ enhancement. The UAPF helps to sustain a stable and reliable power supply, ultimately benefiting industrial operations by reducing equipment malfunctions and improving energy efficiency.

The power supply, series and shunt APF independently control the power flow and the UAPF's mathematical modelling is examined. The Kirchhoff's law supplies the load is explained in the equation (1) and (2) given as follows,

$$V_{abc} = V_s - L_s \frac{di}{dt} - R_s i_{line} - V_{osr} \quad (1)$$

$$i_{line} = i_L - i_{sh} \quad (2)$$

Here, V_s represents the source voltage, V_{abc} indicates phase voltage of power system, V_{osr} represents the output voltage of series APF, i_{line} indicates the line current, i_{sh} denotes the shunt of APF, i_L specifies the load current respectively.

The following equations (3) and (4) indicates the voltage injected by series APF,

$$V_{inj,sr} = V_{Lref} - V_t = -V_L K < 0 \quad (3)$$

$$K = \frac{V_t - V_L}{V_L} \quad (4)$$

Here, to regulate voltage swell and sag, the APF are used, $V_{inj,sr}$ specifies the injected voltage from series APF, V_{Lref} indicates the reference load voltage, the oscillation of source voltage indicated as K, V_t denotes the terminal voltage and $\cos\emptyset_L$ represents the power factor load as computed in equation (5).

$$i_s = \frac{i_L}{1+K} cos\emptyset_L \quad (5)$$

The equation (6) and (7) expressed the power absorbed by the series and shunt APF,

$$S_{sr} = P_{sr} + jQ_{sr} \quad (6)$$

$$S_{sh} = V_L * i_{sh} \quad (7)$$

Here, $P_{sr} = V_{sr} * i_s * \cos\emptyset_s$

$$Q_{sr} = V_{sr} * i_s * sin\emptyset_s \quad (8)$$

From equation (8), i_{sh} indicates difference between the current source and load current, Q_{sr} and P_{sr} represents the reactive power and real/active of the series APF. The following section discusses about the Cascaded Fuzzy controller for regulating the UAPF.

3.2. Modelling of Cascaded Fuzzy Controller

A cascaded Fuzzy controller is a sophisticated control system utilized for managing UAPF, which is crucial in PQ enhancement applications. The cascaded controller enhances the UAPF's performance by dynamically adjusting its parameters based on real time conditions, thereby ensuring effectual operation under varying load and network conditions. The developed controller typically consists of two main control loops such as inner and outer loops. The outer loop responsible for producing the reference currents or voltages based on the desired performance criteria such as harmonic suppression or PFC. The inner loop then adjusts the control signals to achieve these reference values.

The control signal is expressed in equation (9),

$$\Delta u(t) = \sum_{i=1}^{N} \Delta u_i(t) \quad (9)$$

Where, $\Delta u_i(t)$ indicates the change in control signal for each fuzzy rule i.

By utilizing the fuzzy logic, each $\Delta u_i(t)$ is calculates in equation (10),

$$\Delta u_i(t) = \frac{\sum_{j=1}^{M} \mu_{i,j}(e(t)).\Delta u_{i,j}}{\sum_{j=1}^{M} \mu_{i,j}(e(t))} \quad (10)$$

Here, error signal is $e(t)$ and membership function is $\mu_{i,j}$.

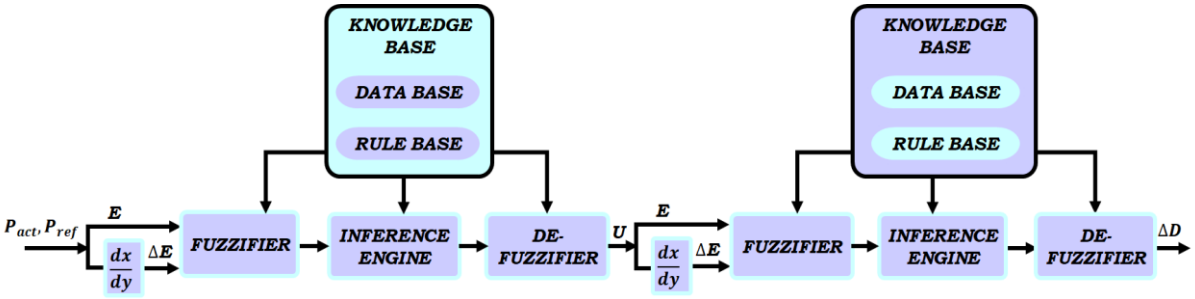


Fig. 4. Cascaded fuzzy controller.

Moreover, the fuzzy logic enables the cascaded fuzzy controller to handle the complex, non-linear dynamics of power systems effectively as illustrated in Figure 4. The following points explains how the fuzzy logic is applied in the context of controlling the UAPF's.

- **Fuzzy Rule base:** A set of linguistic rules is defined to map the input error signal and other system parameters like load conditions to appropriate changes in the control signals.
- **Membership Functions:** this quantify the degree to which belongs to each linguistic variable defined in the fuzzy rule base. These functions capture the uncertainty and vagueness inherent in real world measurements and system responses.
- **Defuzzification:** after evaluating the fuzzy rules, the output fuzzy sets are combined to determine the crisp control action. This process ensures that the controller's decision are clear and actionable within the physical constraints of the UAPF.

Subsequently, the PWM generator (DQ theory) receives the control signals from the cascaded fuzzy controller to generate the appropriate PWM pulses for the UAPF. Furthermore, to power the dc-link of UAPF, the PV system is employed, which convert sunlight into electricity as described as below.

3.3. Modelling of PV System

The PV array model is made up of parallel strings of modules, each string consisting of modules linked in series combination. The equivalent circuit of PV system is represented in Figure 5.

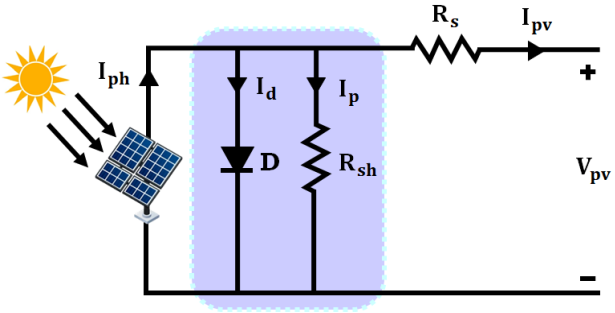


Fig. 5. Circuit diagram of PV system.

The PV system's mathematical model is provided via the equations (11), (12) and (13),

$$I_p = GI_{hg} - i_o exp\left(\frac{q}{nTK_b}\left(V_p + I_p R_{sg}\right) - 1\right) - \left(\frac{V_p + I_p R_{sg}}{R_{shg}}\right) \quad (11)$$

$$i_{ph} = \left(i_{sc} + k_i(T - T_r)\right) \quad (12)$$

$$i_o = exp\left[\frac{qE_g}{Ak_b}\left(\frac{1}{T_r+273} - \frac{1}{T+273}\right)\right]\left(\frac{T+273}{T_r+273}\right) i_r^{\ 3} \quad (13)$$

Here, G specifies SI in W/m^2, number of panels are denoted as n, K_b specifies the Boltzmann constant, R_{sh} and R indicates resistances, q specifies the charge of electron, T and T_r represents the temperature's, E_g denotes the saturation current, and the i_{ph} indicates the hot-generated current. Moreover, to maximize the output power of PV system, the proposed work introduced a novel high gain integrated Boost-Luo converter.

3.4. Modelling of Boost-Luo Converter

The integrated high gain Boost and Luo converter is type of DC-DC converter that combines the topologies of a boost converter and Luo converter as illustrated in Figure 6. This integration allows the converter to achieve high voltage gain from with reduced switching stress. Moreover, there is a reduction in the input filter capacitors current stress and magnitude. There are two modes in this converter as demonstrated in Figure 7. The proposed converter has s switch, 4 diodes, capacitors and an inductor.

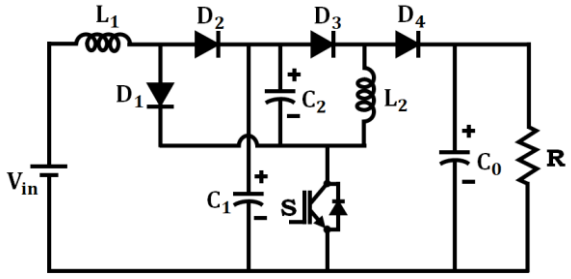


Fig. 6. Circuit diagram of high gain Boost-Luo converter.

Mode 1: When the switch conducts in the first operation mode Figure.7. (a), the forward bias of the first and third diodes become active. In the meantime positive voltage of the magnetized inductors are resent. Due to their negative current, the converter's first and output capacitors are discharged, while its second capacitor has been charged as a result of its positive current.

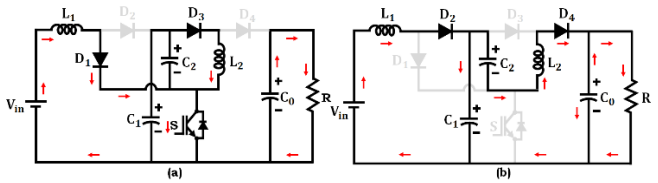


Fig. 7. Modes of operation for integrated Boost-Luo converter (a) Mode 1 and (b) Mode 2.

Mode 2: The switch is on OFF position in this mode, the first and third diodes are biased in the other direction. Conversely, the current begins to flow via the second and fourth diodes. This converter's circuit is shown in Figure 7(b), inductor get a negative voltage. The result is a demagnetized of inductors. Both the input and output capacitors currents are now positive and charging.

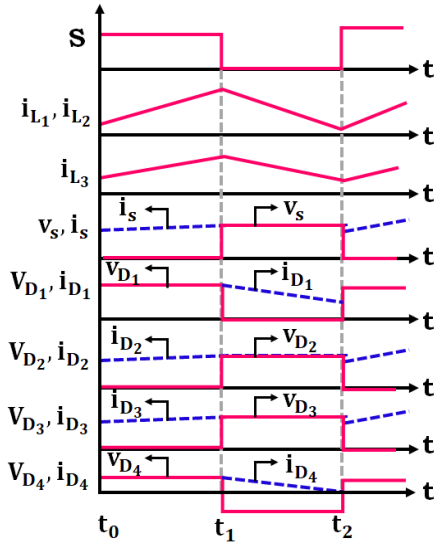


Fig. 8. Switching waveform of Boost-Luo converter.

The equation (14) describe the capacitor current and inductor voltage,

$$\begin{cases} L_1\frac{diL_1}{dt} = v_{in}D + (v_{in} - v_{c1})(1-D), L_2\frac{diL_2}{dt} = v_{c1}D + (2v_{c1} - v_o)(1-D) \\ C_1\frac{dvC_1}{dt} = -(iL_1 + ic_2)D + iL_1 - ic_2)(1-D), C_2\frac{dvC_2}{dt} = ic_2D - iL_2(1-D) \\ C_O\frac{dvC_o}{dt} = -i_oD + (iL_2 - i_o)(1-D) \end{cases} \quad (14)$$

The equation (15) for the average voltage of the capacitors and average current of the inductor is given as below.

$$\begin{cases} Vc_1 = \frac{v_{in}}{1-D}, Vc_2 = \frac{v_{in}}{1-D}. Vc_o = \frac{(2-D)v_{in}}{(1-D)^2} \\ IL_1 = \frac{(2-D)}{(1-D)^2}I_o, IL_2 = \frac{1}{1-D}I_O \end{cases} \quad (15)$$

The current flowing through the inductors when the semiconductors are in their active models causes the current stress in the switch as well as diodes. The capacitors voltage and the semiconductors inactive mode is the cause of voltage stress on the semiconductors. The relationship between the input voltage, output current and duty cycle used to express the voltage/current stress of semiconductors are related in equation (16),

$$\begin{cases} IS_1 = \frac{(1+D-D^2)Io}{(1-D)^2}, ID_1 = \frac{D(2-D)I_O}{(1-D)^2}, ID_2 = \frac{(2-D)Io}{1-D}, ID_3 = ID_4 = I_O \\ VS_1 = VD_3 = VD_4 = \frac{V_{in}}{(1-D)^2}, VD_1 = \frac{DV_{in}}{(1-D)^2}, VD_2 = \frac{V_{in}}{1-D}, \end{cases} \quad (16)$$

Timing diagram of proposed high gain-boost luo-converter is displayed in Figure 8. By utilizing this converter, the output voltage of PV is efficiently boosted with better voltage gain and reduced switching stress. Moreover, to stabilize the voltage with better convergence rate, the improved artificial rabbit optimized PI controller is utilized as discussed below.

3.5. Modelling of Improved Artificial Rabbit Optimization

The improved ARO is developed for tuning the parameters for PI controller. This optimization method enhances the traditional ARA by incorporating an adaptive exploration and exploitation mechanism, which dynamically balances the search of new optimal solution and the refinement of existing ones. In this work, to enhance the efficiency of the conventional ARA. The Adaptive Local Search (ALS) and Experience Based Perturbation Learning (EPL) are the foundation of the enhanced IARO. When a rabbit is in the exploration phase, it follows the rabbit in the population. Invasive diversification patterns result from this update schedule. In order to enhance the exploratory search the EPL is incorporated to find the locations inside the workable search space. Specifically, the EPL begins by computing the mean $\Delta^{it}{}_{mean}$ and deviation $\Delta^{it}{}_{dev}$ of every randomly selected solution in relation to the best solution Δ_{best} . Subsequently, the modified answer is made based on the development with the distributed term. As a result, the improved solution is expressed in equations (17)-(21),

$$\Delta^{it}{}_{mean} = (Z_{best} + z^{it}{}_I)/2 \quad (17)$$

$$\Delta^{it}{}_{dev} = abs(Z_{best} - z^{it}{}_I) \quad (18)$$

$$\Delta^{it}{}_C = \Delta^{it}{}_{mean} + rand_1.\Delta^{it}{}_{dev} \quad (19)$$

$$z^{it}{}_{new} = \Delta^{it}{}_C + rand_2.(Z_{best} - \Delta^{it}{}_C) + 0.95^{it}.(rand_3 - 0.3).abs(z_{max,j} - z_{min,j}), z_{max,j} \quad (20)$$

$$= max_j\{z_i{}^{it}\}, z_{max,j} = min_j\{z_i{}^{it}\}\forall I \quad (21)$$

Where, $\Delta^{it}{}_I$ specifies the arbitrary solution select at random, $rand_1, rand_2, rand_3$ denotes the random numbers based on the interval [0, 1].

An ALS strategy is said to be a guidance system based on shared information over elite group within the rabbits along with their best individual Z_{best} and the worst be individual Z_{worst}, with the goal of reducing the loss of accuracy at the iterative process as well as enhancing exploitation near the promising space. Specifically, the method that determines the best and worst role with in this group and the elite group based on fitness function(z^p and z^w). The updating stage is then carried out using three different sorts of the movement's using z^w in the direction of z^p and pushing z^win the direction of medium of z^p andZ_{best} . These activates are done after the other in a

sequential manner, which ending when a particular person reaches a higher level of fitness. The equation (22) is an expression of this strategy's updating phase,

$$\begin{aligned} Z^{ALS}{}_1 &= 2 \times r_1 \times (z^p - z^w) + z^w \\ Z^{ALS}{}_2 &= 2 \times r_2 \times (Z_{best} - z^w) + z^w \\ Z^{ALS}{}_3 &= 2 \times r_3 \times (z^p + Z_{best})/2 - z^w + z^w \end{aligned} \qquad \begin{aligned} Z^{it+1}{}_I = \\ if\ f(Z^{ALS}{}_I) \le f(Z^{it}{}_I) \\ else\ if\ f(Z^{ALS}{}_2) \le f(Z^{it}{}_I) \\ otherwise \end{aligned} \tag{22}$$

Here, $z^{it}{}_I$ and $Z^{it+1}{}_I$ denotes the current and improved solutions of ith solution in an elite class. The flowchart for this improved ARO is represented in Figure 9 as follows. The developed Improved ARO algorithm efficiently tuned the PI controller with precise voltage regulation and rapid convergence speed.

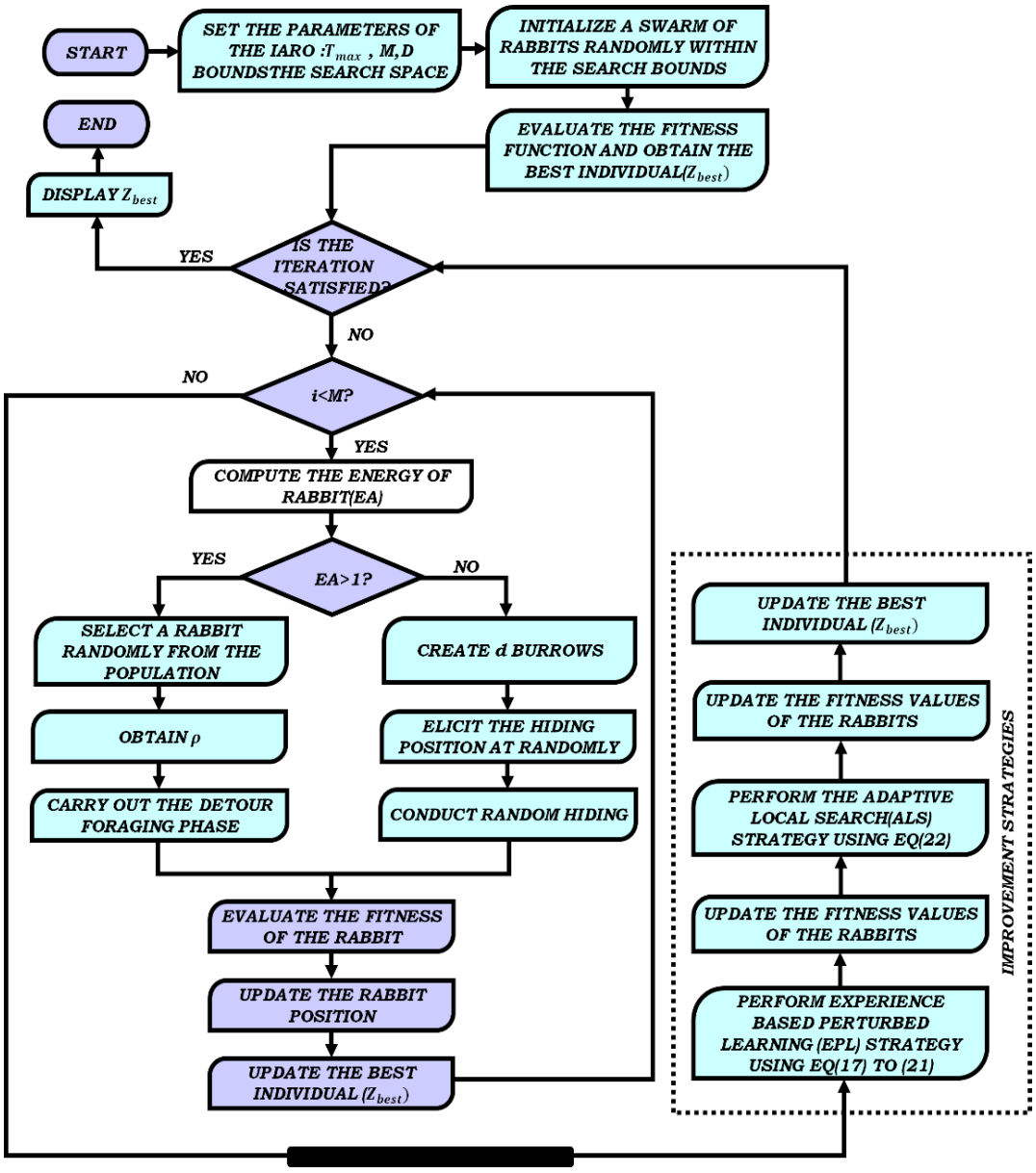


Fig. 9. Flowchart of improved ARO.

Consequently, the stabilized voltage is deliver to the PWM generator for producing pulses for the better switching operation of the converter. Finally, the enhanced and stabilized voltage is given to the linear and non-linear load via the UAPF system.

4. Results and Discussion

High PQ is crucial for maintaining the operational efficiency and longevity of electrical equipment. Thus, the UAPF is employed in this work, which mitigate PQ issues in linear and non-linear load system by combining the functionalities of series and shunt APF. The cascaded Fuzzy controller is used to enhance the effectiveness of UAPF for enabling adaptive and predictive control responses, thereby the harmonic compensation, reactive power control and voltage regulation is attained. Furthermore, the PV system with integrated Boost-Luo converter based Improved ARO based PI controller power the DC-link of UAPF, which

provides enhanced power supply require for the linear and non-linear load. To evaluate the performance of the developed system, MATLAB/Simulink is deployed. The outcomes obtained for the developed work is illustrated in this section with the comparative analysis. Table 1 specifies the parameter specification for the developed work.

Table 1 Parameter specification

Parameter	Specification
AC Source	
Load Resistance	100Ω
Load Inductance	10mH
PV system	
Open circuit voltage	22.6V
Short circuit voltage	12A
Integrated Boost-Cuk converter	
L_1, L_2	$1mH$
C_1, C_2	$4.7\mu F$
C_0	$2200\mu F$
Switching Frequency	$10kHz$

a) Case 1 with step magnitude -0.2

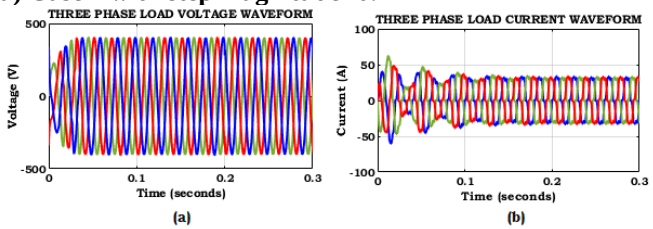


Fig. 10. Three phase load waveform.

The three phase load voltage waveform is illustrated in Figure 10(a) and (b), which indicates that the voltage and current fluctuates initially and after it constantly stabilized at 415V and 30A. The UAPF quickly respond to the sag event by compensating for the drop in voltage and ensures the current supplied to the load remains stable and free of significant distortion.

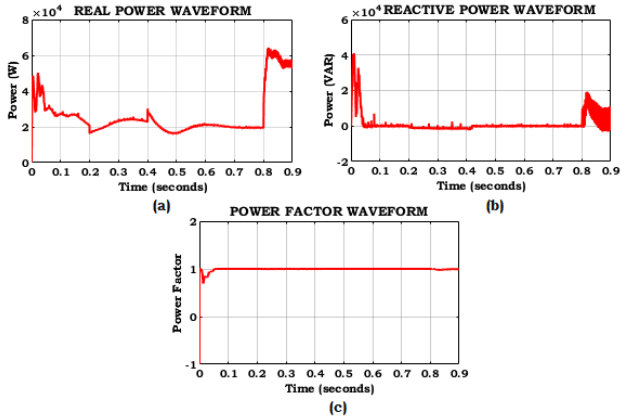


Fig. 11. (a) Real power (b) Reactive power and (c) Power factor waveform.

The real and reactive power waveform illustrated in Figure 11(a) and (b) indicating active compensation and management to handle varying load conditions, the reactive power is actively managed by compensating device such as UAPF. Additionally, the power factor waveform demonstrates that the system's ability to preserve efficient power utilization and it remains close to 1 for the time interval with minor oscillations as specified in Figure 11(c).

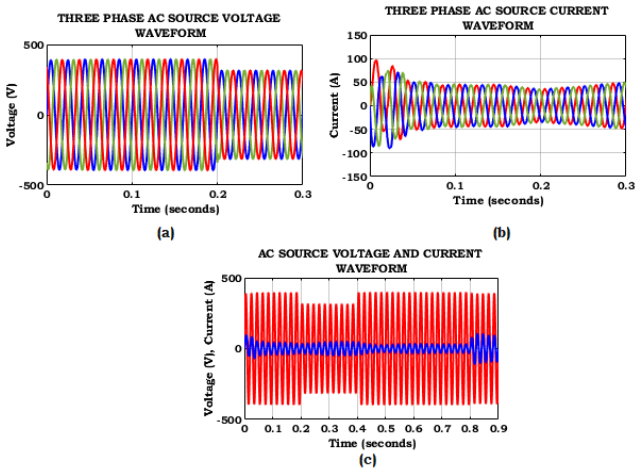


Fig. 12. Three phase AC source waveform (a) Voltage (b) Current waveform and (c) Voltage and current waveform.

The three phase AC source waveform for the voltage is represented in Figure 12(a), which provide the stabilized voltage of 415V and the current waveform in Figure 12(b) specifies that current gets highly oscillated in initial period and after 0.25s it constantly stabilized at 45A. Moreover, the in phase waveform for the AC source is specified in Figure 12(c), the voltage and current is stabilized without any distortions respectively.

The DC-link voltage waveform is illustrated in Figure 13, in which the blue line indicates the reference voltage, which exhibits fluctuations, likely due to the changes in power demand or load conditions. Similarly, the red line indicates the actual voltage waveform observed on the DC link, which closely tracks the reference waveform, with some deviations it gets constant voltage at 850V respectively.

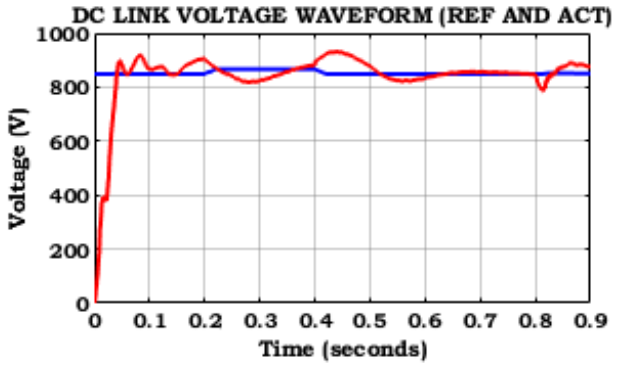


Fig. 13. DC-link voltage waveform.

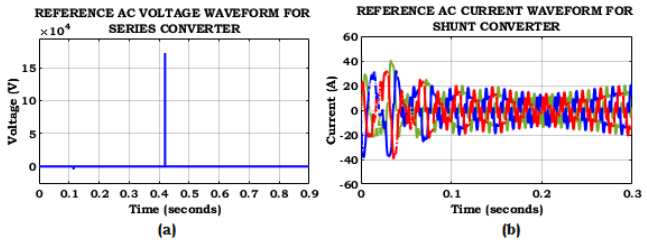


Fig. 14. Reference AC waveform (a) voltage for series converter and (b) Current for shunt converter.

Fig. 14 demonstrates the reference AC voltage and current waveform for the series and shunt converter. The series converter waveform represents that the voltage of the converter as displayed in Figure 14(a) achieve the desired power flow. The Figure 14(b) represents the AC current waveform for the shunt converter. By coordinating the operation of these two converters, the UAPF approach achieve efficient and flexible power flow management.

b) Case 2 with step magnitude -0.2

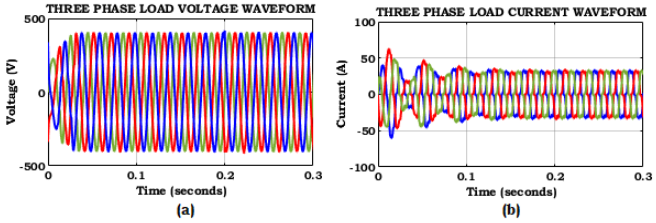


Fig. 15. Three phase Load waveform for case 2.

Fig. 15(a) and (b) represents the three phase load voltage waveform, which shows that the voltage and current vary at first, then steadily stabilized at 415V and 30A. In order to ensure the current delivered to the load is stable and free of sustainable distortion, the UAPF promptly responds to the swell event by compensating for the voltage drop.

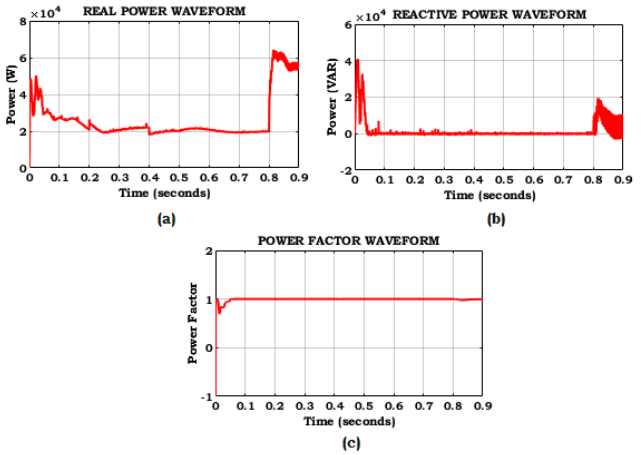


Fig. 16. (a) Real power (b) Reactive power and (c) Power factor waveform.

Fig. 16(a) and (b) depict the real and reactive power waveforms, which show active reactive power management and compensation to handle varying load situations. A compensating device like UAPF actively manages reactive power. Furthermore, the power factor waveform shows that the system continue to use power efficiently and stays near to 1 during the period of time with slight oscillations as shown in Figure 16(c).

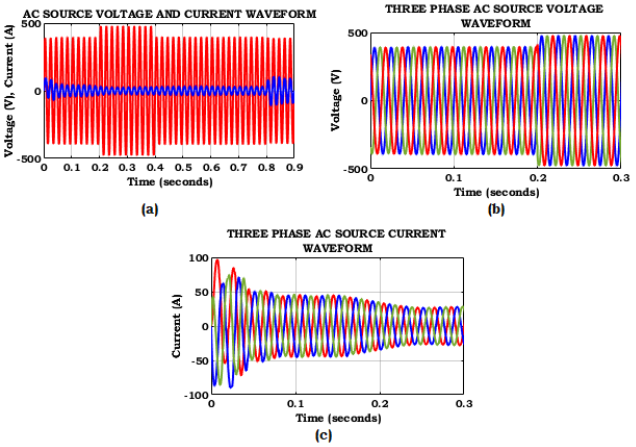


Fig. 17. Three phase AC source waveform (a) Voltage and current (b) voltage and (c) Current waveform.

Fig. 17(a) shows the in phase waveform for the AC source, which illustrates there are the stabilized voltage and current. Figure 17(b) shows the three-phase AC source waveform for the voltage, which provides a stabilized range at 415V. Figure 17(c) shows the current waveform, which indicates that the current oscillates greatly in the beginning and then steadily stabilizes at 45A after 0.25 seconds

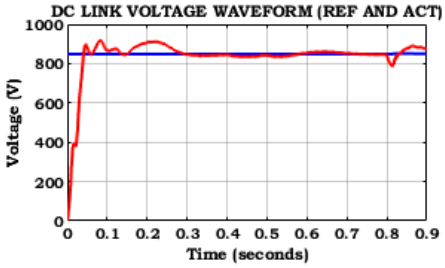


Fig. 18. DC-link voltage waveform.

In Figure 18, the DC-link voltage waveform is depicted, the reference voltage, represented by the blue line, which varies as a result of variations in load circumstances or power demand. Comparably, the red line shows the real voltage waveform seen on the DC link, which mostly follows the reference waveform and reach a constant value of 850V, respectively.

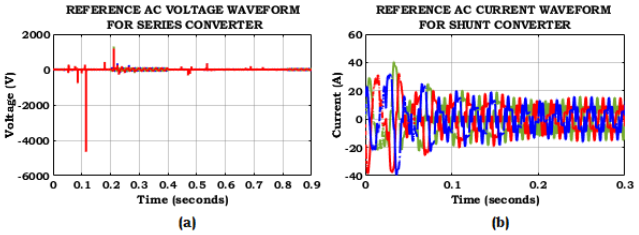


Fig. 19. Reference AC waveform (a) voltage for series converter and (b) Current for shunt converter.

The reference AC voltage and current waveform for the series and shunt converter is shown in Figure 19. The series

converter waveform from Figure 19. (a) shows that the converter's voltage produces the intended power flow. The shunt converter's AC current waveform is shown in Figure 19(b), through the synchronization of these two converters, the UAPF method accomplishes effective and adaptable power flow control.

Figure 20 shows the THD waveform for current attained by the developed work, which is observed that the proposed Cascaded ANN controller attains the THD value of 0.98%, thereby effectively mitigating the PQ disturbances.

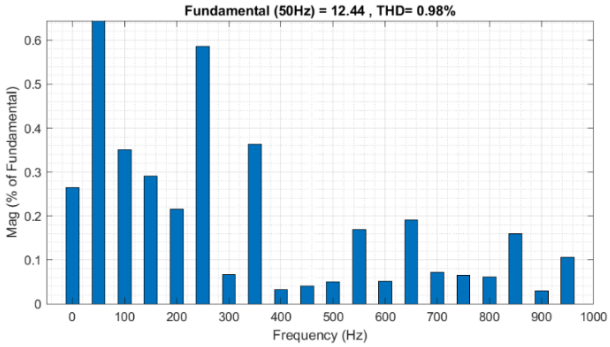


Fig. 20. THD waveform.

Table 2. Comparison of Proposed UAPF (Cascaded Fuzzy controller) with conventional control approach

SI. No	Features	UPQC (SRF controller) [24]	UPQC (ANN controller)[25]	UAPF (Cascaded Fuzzy controller)
1.	Complexity	High	low	**Very low**
2.	Dynamic response	low	High	**High level**
3.	Accuracy	low	Medium	**High level**
4.	Process of Controlling	Slower	Fast	**Very High**
5.	% THD	3.56%	2.97%	**0.98%**

Table 2 shows that the proposed UAPF with cascaded fuzzy control is a much better option than the conventional SRF and ANN-based controller. A cascaded fuzzy controller has the advantage of keeping complexity low without compromising the dynamic response and accuracy, which are very important for the real-time PQ improvement. Most significantly, the proposed method bring down the THD to 0.98%, which is far below the limit set by the IEEE-519 standard, thus proving its capability in harmonics reduction. Such a massive drop in THD level lead to system stabilization, less energy wastage and longer equipment life.

Fig. 21 illustrates voltage gain of the integrated Boost-proposed converter constantly produces higher voltage gain than other converters, which proves its appropriateness for the PV-based systems where stable and high voltage level is required.

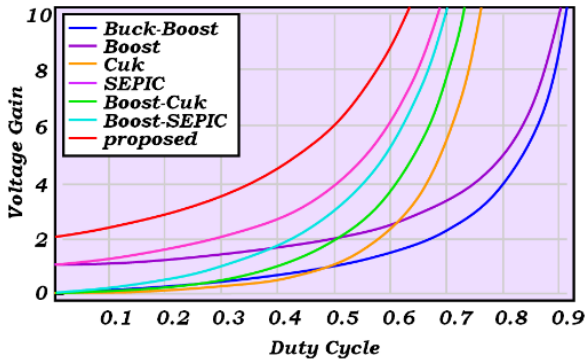


Fig. 21. Comparison of voltage gain.

Table 3. Comparison of traditional converters [20] with the proposed Boost-Luo converter

Converters	Inductors	Capacitors	Switches	Diodes	Input resistance	Voltage gain	Switching loss
Boost	1	1	1	1	$(1-D)^2 R_L$	$\frac{1}{1-D}$	High
Buck-Boost	1	1	1	1	$\frac{(1-D)^2}{D^2} R_L$	$\frac{D}{1-D}$	Low
Cuk	2	1	1	1	$\frac{(1-D)^2}{D^2} R_L$	$-\frac{D}{1-D}$	Low
SEPIC	2	1	1	1	$\frac{(1-D)^2}{D^2} R_L$	$\frac{D}{1-D}$	Low
Proposed Boost-Luo	2	3	1	3	$\frac{(1-D)^2}{D^2} R_L$	$\frac{SD-1}{2D-1}$	Very Low

Table 3 illustrate that the proposed BoostLuo converter has a greater voltage gain than the conventional converters and at the same time switching losses have been reduced. This is a major upgrade for PV systems whose output is low and intermittent which needs to be efficiently boosted and stabilized. The converter's structure lowers the stress of switching devices and enhances efficiency. Thus, the Boost-Luo converter is a more dependable and environmentally friendly option for renewable energy integration.

Fig. 22 depicts the MSE value comparison among three optimization algorithms such as IARO, Artificial Rabbit Optimization (ARO) and Particle Swarm Optimization (PSO). It indicates that IARO mainly obtains lower MSE values than other algorithms at different iterations, thus outperforming both ARO and PSO in terms of convergence rate and error reduction.

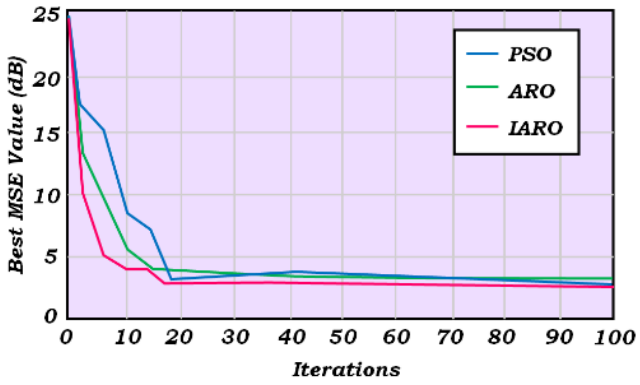


Fig. 22. Comparison of best MSE value.

5. Conclusion

This paper proposes UAPF integrated with the High gain Integrated Boost-Luo converter for PQ enhancement. The UAPF effectively mitigates PQ issues like harmonics, reactive power and load unbalance in linear and non-linear loads. By employing a Cascaded Fuzzy controller, the UAPF achieves superior control accuracy and robustness in managing harmonic current. The UAPF integration with High gain Integrated Boost-Luo converter enhances the output voltage of PV efficiently with high voltage gain ratio and reduced switching stress. Moreover, the utilization of an Improved ARO optimized PI controller, which allowing for precise control and adaptive tuning performance, thereby providing the overall system stability with reduced MSE error. The MATLAB/Simulink is implemented for analyzing the proposed system effectiveness and the comparative analysis outcomes demonstrates that the proposed system attains better dynamic response, reduced THD value of (0.98%), high voltage gain and minimized MSE compared to the traditional approaches. Thus, the proposed system not only addresses current PQ issues effectively but also paves the way for future enhancement in renewable energy integration and load stability.

Acknowledgements

Not applicable.

Author Contributions

K. Natarajan: Conceptualization, Methodology, Writing-Original Draft

Mohammadha Hussaini M, Siddheswar Kar, Krishna Prakash Arunachalam: Data Curation, Methodology, Supervision

Pranita Chavan, S. Baskaran: Project administration, Validation, Writing - Review & Editing

All authors reviewed and approved the final version.

Conflict of Interest

The authors declare no conflict of interest.

References

[1] P. S. Sanjan, N. Gowtham, M. S. Bhaskar, U. Subramaniam, D. J. Almakhles, S. Padmanaban, and N. G. Yamini, “Enhancement of power quality in domestic loads usin0g harmonic filters”, IEEE Access, vol. 8, pp. 197730-197744, Oct. 2020, doi: https://doi.org/10.1109/ACCESS.2020.3034734

[2] A. Y. Qasim, F. R. Tahir, and A. N. B. Alsammak, “Utilizing UPQC-Based PAC-SRF techniques to mitigate power quality issues under non-linear and unbalanced loads”, Journal Européen des Systèmes Automatisés, vol. 56, no. 5, Oct. 2023.

[3] P. Sujidha, M. Devi, A. Manjula, N. Thillainayagi, and A. Usha, “Novel approach of power quality issues suppression using cascaded h-bridge multilevel inverter based DSTATCOM”, Int. J. Adv. Res. Sci. Commun. Technol, 2022.

[4] K. Hasan, M. M. Othman, S. T. Meraj, M. Ahmadipour, M. H. Lipu, and M. Gitizadeh, “A unified linear self-regulating method for active/reactive sustainable energy management system in fuel-cell connected utility network”, IEEE Access, vol. 11, pp. 21612-21630, Feb. 2023, doi: https://doi.org/10.1109/ACCESS.2023.3249483

[5] S. J. Alam, and S. R. Arya, “Control of UPQC based on steady state linear Kalman filter for compensation of power quality problems”, Chinese Journal of Electrical Engineering, vol. 6, no. 2, pp. 52-65, Jun. 2020, https://doi.org/10.23919/CJEE.2020.000011

[6] S. G. Reddy, S. Ganapathy, and M. Manikandan, “Three phase four switch inverter based DVR for power quality improvement with optimized CSA approach”, IEEE Access, vol. 10, pp. 72263-72278, Jul. 2022, doi: https://doi.org/10.1109/ACCESS.2022.3188629

[7] E. Akbari, and A. Z. G. Seyyedi, “Power quality enhancement of distribution grid using a photovoltaic based hybrid active power filter with three level converter”, Energy Reports, vol. 9, pp. 5432-5448, Dec. 2023, doi: https://doi.org/10.1016/j.egyr.2023.04.368

[8] S. Chandrakala Devi, B. Singh, and S. Devassy, "Modified generalised integrator based control strategy for solar PV fed UPQC enabling power quality improvement", IET Generation, Transmission & Distribution, vol. 14, no. 16, pp. 3127-3138, Aug. 2020, doi: https://doi.org/10.1049/iet-gtd.2019.1939

[9] T. Ravi, and K. Sathish Kumar, "Analysis, monitoring, and mitigation of power quality disturbances in a distributed generation system", Frontiers in Energy Research, vol. 10, pp. 989474, Nov. 2022, doi: https://doi.org/10.3389/fenrg.2022.989474

[10] M. Golla, S. Thangavel, S. P. Simon, and N. P. Padhy, "A novel control scheme using UAPF in an integrated PV grid-tied system", IEEE Transactions on Power Delivery, vol. 38, no. 1, pp. 133-145, Jun. 2022, doi: https://doi.org/10.1109/TPWRD.2022.3180681

[11] M. Aijaz, I. Hussain, S. A. Lone, and M. Chankaya, "GRLF-LAD control based active power filter operation with QSG-SOGI algorithm for grid voltage harmonics disturbance rejection", IEEE Access, vol. 11, pp. 135753-135763, Nov. 2023, doi: https://doi.org/10.1109/ACCESS.2023.3337551

[12] A. M. Bloul, M. Abuhamdah, A. M. Sharaf, H. H. Aly, and J. Gu, "An efficient shunt modulated AC green plug-switched filter compensation scheme for nonlinear loads", Energies, vol. 17, no. 10, pp. 2426, May. 2024, doi: https://doi.org/10.3390/en17102426

[13] M. A. Hannan, G. Sebastian, A. Q. Al-Shetwi, P. J. Ker, S. A. Rahman, M. Mansor, K. M. Muttaqi, and M. Uddin, "Particle swarm optimization algorithm based fuzzy controller for solid-state transfer switch toward fast power transfer and power quality mitigation", IEEE Transactions on Industry Applications, vol. 59, no. 5, pp. 5570-5579, Jun. 2023, doi: https://doi.org/10.1109/TIA.2023.3289440

[14] T. Ravi, K. S. Kumar, C. Dhanamjayulu, B. Khan, and K. Rajalakshmi, "Analysis and mitigation of PQ disturbances in grid connected system using fuzzy logic based IUPQC", Scientific Reports, vol. 13, no. 1, pp. 22425, Dec. 2023, doi: https://doi.org/10.1038/s41598-023-49042-z

[15] S. Parthiban, and V. Madhaiyan, "Experimental validation of solar PV sustained ZSI based unified active power filter for enrichment of power quality", Automatika, vol. 62, no. 1, pp. 137-153, Jan. 2021, https://doi.org/10.1080/00051144.2021.1908013

[16] S. S. Dheeban, and N. B. Muthu Selvan, "ANFIS-based power quality improvement by photovoltaic integrated UPQC at distribution system", IETE Journal of Research, vol. 69, no. 5, pp. 2353-2371, Jul. 2023, doi: https://doi.org/10.1080/03772063.2021.1888325

[17] B. N. Reddy, F. Alsaif, C. R. Reddy, and S. S. Kumar, "Development of multiple input supply based modified SEPIC DC–DC converter for efficient management of DC microgrid", Scientific Reports, vol. 14, no. 1, pp. 11066, May. 2024, doi: https://doi.org/10.1038/s41598-024-61713-z

[18] W. El Aouni, and L. A. Dessaint, "Real-time implementation of input-state linearization and model predictive control for robust voltage regulation of a DC-DC boost converter", IEEE Access, vol. 8, pp. 192101-192108, Oct. 2020, doi: https://doi.org/10.1109/ACCESS.2020.3032327

[19] S. Prakash, M. Alkhatib, H. F. Sindi, S. Alghamdi, R. K. Behera, and U. R. Muduli, "Adaptive control for shunt active power filter under stochastic solar photovoltaics behavior", IEEE Journal of Emerging and Selected Topics in Power Electronics, vol. 13, no. 3, pp. 3673-3687, 2025. https://doi.org/10.1109/JESTPE.2025.3525489

[20] S. Coelho, V. Monteiro, T. J. Sousa, L. A. Barros, D. Pedrosa, C. Couto, and J. L. Afonso, "A unified power converter for solar PV and energy storage in dc microgrids", Batteries, vol. 8, no. 10, pp. 143, 2022. doi.org/10.3390/batteries8100143

[21] R. Boopathi, and V. Indragandhi, "Enhancement of power quality in grid-connected systems using a predictive direct power controlled based PV-interfaced with multilevel inverter shunt active power filter", Scientific Reports, vol. 15, no. 1, pp. 7967, 2025. https://doi.org/10.1038/s41598-025-92693-3

[22] V. Sheeja, R. Kalpana, U. Subramaniam, and D. J. Almakhles, "Control of converter for a solar PV-BESS powered telecom load with real, reactive and harmonic power exchange with grid", IEEE Access, vol. 11, pp. 141008-141021, 2023. https://doi.org/10.1109/ACCESS.2023.3340433

[23] K. Hemasri, and C. S. Kumar, "Fuzzy controller with shunt active power filter in reducing THD for three phase system", International Transactions on Electrical Engineering and Computer Science, vol. 3, no. 2, pp. 101-108, 2024. https://doi.org/10.62760/iteecs.3.2.2024.93

[24] H. Mahar, H. M. Munir, J. B. Soomro, F. Akhtar, R. Hussain, M. F. Elnaggar, S. Kamel, and J. M. Guerrero, "Implementation of ANN controller based UPQC integrated with microgrid", Mathematics, vol. 10, no. 12, pp. 1989, Jun. 2022, doi: https://doi.org/10.3390/math10121989

[25] R. Gopalasami, B. Chokkalingam, and S. Muthusamy, "A novel method for hybridization of super lift luo converter and boost converter for electric vehicle charging applications", Energy Sources, Part A: Recovery, Utilization, and Environmental Effects, vol. 45, no. 3, pp. 8419-8437, Aug. 2023, doi: https://doi.org/10.1080/15567036.2023.2226104